

# Seismotectonics of the 2001 Bhuj earthquake (M<sub>w</sub> 7.7) in western India: Constraints from aftershocks

J.R. Kayal<sup>1</sup> and S. Mukhopadhyay<sup>2</sup>

1. Geological Survey of India, 27, J.L. Nehru Road, Kolkata – 700 016 • email: jr\_kayal@hotmail.com  
2. Department of Earth Sciences, IIT Roorkee, Roorkee 247 667, India

---

## ABSTRACT

More than 500 aftershocks ( $M > 2.0$ ) are relocated to study the source processes of the January 26, 2001 Bhuj earthquake ( $M_w 7.7$ ) in western part of the peninsular Indian shield. The maximum intensity reached to X on the MSK scale, but no primary surface rupture or fault was mapped. The aftershocks are relocated by simultaneous inversion with an average rms of 0.19s, and average error estimates of latitude, longitude and depth are 1.2 km, 1.1 km and 2.3 km, respectively. Most of the aftershocks occurred in an area of 70 x 35 sq km; the maximum activity was observed at a depth range of 12-37 km. A bimodal distribution of aftershocks indicates that the main shock rupture propagated both in the upward and downward directions. Further, the best located larger magnitude aftershocks show two trends, one in northeast, parallel to the isoseismal trend and to the major Anjar Rapar Lineament/Delhi – Aravalli trend, and the other in northwest parallel to the Bhachau Lineament and a 8 km long secondary rupture. Fault-plane solutions of the northeast trending aftershocks indicate reverse faulting with left-lateral strike-slip motion; these are comparable to the main shock mechanism. The northwest trending aftershocks, on the other hand, show reverse faulting with right-lateral strike-slip motion. 3D-velocity, gravity, magnetic, ground positioning system (GPS) and satellite observations suggest block uplift during the main shock. These observations are comparable to the earthquake locations and source mechanisms of the main shock and aftershocks.

---

## INTRODUCTION

The devastating Bhuj earthquake of January 26, 2001, epicentre 23.4°N, 70.28°E, magnitude  $M_w 7.6 + 0.1$  (USGS, ERI) and well estimated focal depth 25 km with Sp depth phases (IMD, 2002) occurred in the Kutch (also called Kachchh) rift basin in the western margin of peninsular India (Fig.1). It attracted attention from national and international research community to understand the source processes of such a deadly intraplate earthquake, and to compare it with the global scenario.

Detailed macroseismic studies were carried out by many investigators (e.g. Ravishanker and Pande, 2001; Wesnousky et al., 2001; Rajendran et al., 2001; Rastogi, 2001; McCaplin and Thakkar, 2001). The maximum intensity was X on the MSK scale, and caused severe damage to properties and claimed about 20,000 human lives (Ravishanker and Pande, 2001).

The aftershock sequence was well recorded by temporary networks deployed by various national organizations, like the Geological Survey of India (GSI,

2003), India Meteorological Department (IMD, 2002), and National Geophysical Research Institute (NGRI) as well as by a few international organizations (e.g. USGS: Horton et al., 2001; Bodin and Horton, 2004 and ERI, Japan: Negishi et al., 2002). In this study, the aftershocks that were recorded by a 12 – station GSI temporary network for about two and a half months, immediately after the main shock (Kayal et al., 2002a), are analysed for relocations, and a detailed study of fault-plane solutions of the aftershocks are made to understand the source processes.

Pre- and post- earthquake gravity, magnetic, ground positioning system (GPS) and satellite observations were also made (e.g. Chandrasekhar et al., 2004; Jade et al., 2002; Gahalaut and Bürgmann, 2004). Further, 3D-velocity structure is studied by Kayal et al. (2002b), Mandal et al. (2004) and Mukhopadhyay and Kayal (2005). All these available data are reviewed in this study to address the seismotectonic implications of the Bhuj earthquake sequence, one of the largest intraplate earthquakes in the recorded history.

**SEISMICITY AND TECTONICS**

The Kutch area falls in the highest seismic zone (Zone V) in the seismic zoning map of India (BIS, 2002). The Kutch, Cambay and Narmada rifts are the three major rift-basins in the western margin of peninsular India craton (Fig.1). These rift-basins are bounded by

three important Precambrian tectonic trends: the NNW-SSE Dharwar trend, the NE-SW Delhi-Aravalli trend and the ENE-WSW Satpura trend (also known as Son Narmada Tapti Lineament or SONATA), which dominate the structural fabric of the region (e.g. Oldham, 1926; Biswas, 1987; Talwani and Gangopadhyay, 2001).

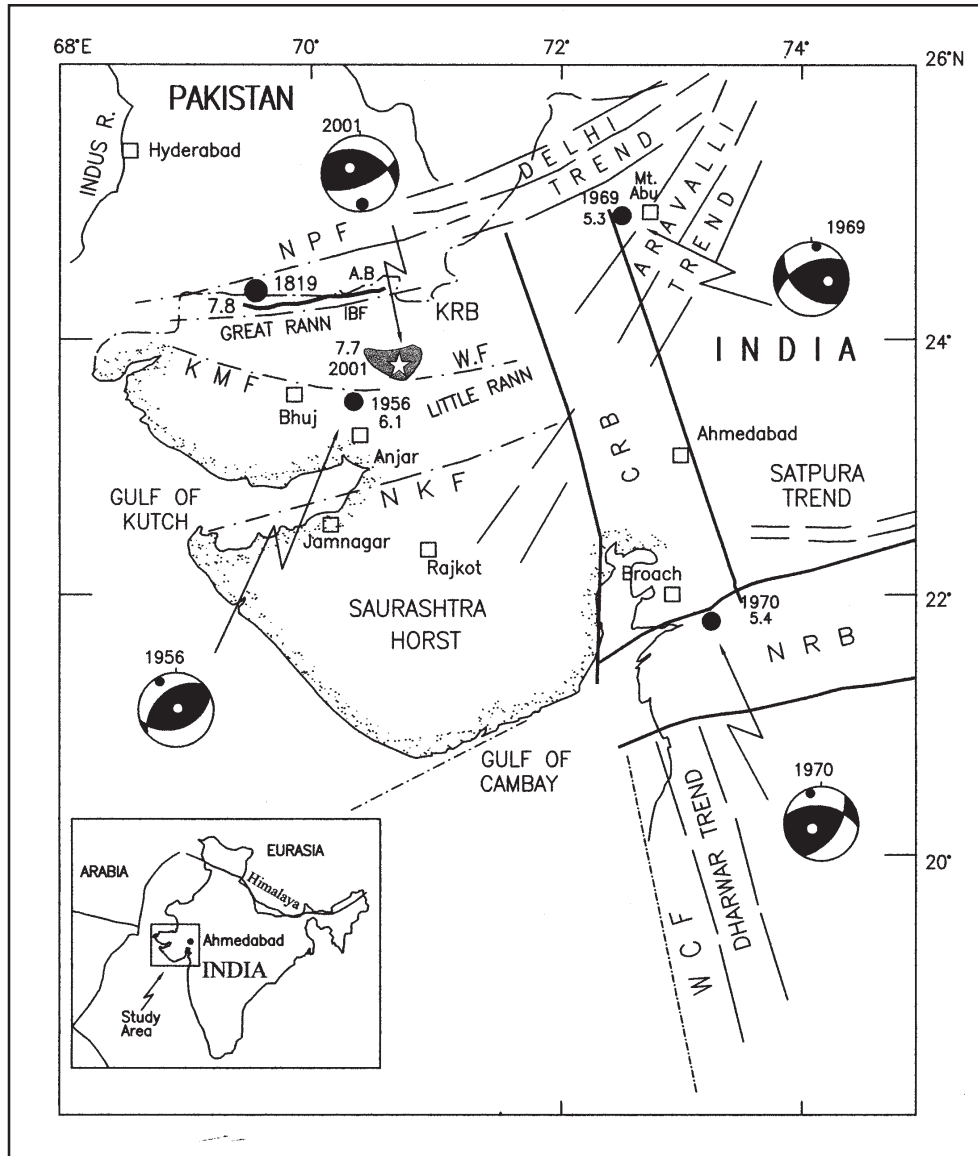


**Figure 1.** The map showing major tectonic features in the study region (compiled by Kayal et al., 2002a). **KRB:** Kutch Rift Basin, **CRB:** Cambay Rift Basin, **NRB:** Narmada Rift Basin, **NPF:** Nagar Parkar Fault, **IBF:** Island Belt Fault, **KMF:** Kutch Mainland Fault, **NKF:** North Kathiwar Fault, **WCF:** West Coast Fault, **AB:** 'Allah Bund' (thicker line), (see text). Epicenters and fault-plane solutions of the past significant earthquakes  $M > 5.0$  are shown. In fault-plane solutions, the solid circle indicates P-axis in the dilatational zone (open area), and the open circle T-axis in the compressional zone (dark area). Epicenter of the 1819 earthquake is given after Rajendran et al. (2001). The open star indicates the epicenter of the main shock of January 26, 2001, and the V-shaped shaded area indicates the aftershock area as reported by Wesnousky et al. (2001). Inset: Indian subcontinent indicating the study area and plate boundary.

In the Kutch region, the tectonic trend is E-W, along which rifting resulted in the formation of the Kutch Rift Basin (KRB). The NE-SW Aravalli trend, on the other hand, continues and across the Cambay basin into Saurashtra horst to form the southwesterly plunging Saurashtra arch. The Cambay Rift Basin (CRB) is considered to have formed along the northern extension of the Dharwar trend. The Narmada Rift Basin (NRB) extends into the Cambay graben, and continues into the southern part of Saurashtra. All the three rift basins along the Precambrian structural trends originated in different periods during the Mesozoic. The Cambay basin, however, though originated during the Mesozoic, subsided at a greater rate during the Tertiary (GSI, 2000).

The Kutch basin, the present study area, is distinguished by E-W oriented high lands (uplifts) and low lying basins or 'Ranns' ('Ranns' mean uninhabited salt flats that are neither sea nor land, and are flooded periodically). A number of E-W faults control the structural trend of the Kutch rift; these are: the Nagar Parkar Fault (NPF), the Allah Bund Fault, the Island Belt Fault (IBF), the Kutch Mainland Fault (KMF) and the North Kathiwar Fault (NKF), (Fig.1). The NPF is the northern boundary and the NKF the southern boundary faults of the KRB. The basin is filled with sediments ranging in age from middle Jurassic to Tertiary. The Deccan trap lavas, late Cretaceous to early Paleocene, divide the Mesozoic and Tertiary stratigraphy of the Kutch basin. After initial period of extension the KRB has been subjected to N-S compression by the resultant back push of the Himalaya at least since 20 ma (Talwani and Gangopadhyay, 2001). The structure of the basin is styled by a series of uplifts, master faults and up-thrusts (Biswas, 1982 and 1987). The uplifts are the results of the differential movements of discrete basement blocks due to compression along these faults. The Bouguer gravity anomaly in the Kutch basin is high and the contours also have the E-W trend (GSI, 2000; Chandrasekhar et al., 2002). In addition to the major E-W faults, the basin is transected by major N-S to NE-SW and NW-SE tectonic lineaments that include a structural 'Median High' (Hinge Zone) to the west of Bhuj, a NE-SW lineament from near Anjar through Rapar (hereafter called A-R lineament), a NW-SE lineament from Bhachau to the NW (hereafter called Bhachau lineament), NW-SE Banni fault and various short lineaments and faults (GSI, 2000; Talwani and Gangopadhyay, 2001), (Fig.2).

Among the past major earthquakes in peninsular India, the largest intraplate event was the June 1819 Kutch earthquake. The maximum intensity was

reported to be XI on MM scale (Oldham, 1926). This earthquake occurred before the existence of any seismograph instrument in the country. Based on the reported intensity, Gutenberg and Richter (1954) assigned  $M_L \sim 8.0$ , whereas Johnston and Kanter (1990) assigned  $M_w = 7.8$ . A remarkable feature of this earthquake was the creation of a 80 to 90 km long elevated tract of land, known as 'Allah Bund' (dam of God), close to the international border between India and Pakistan (Fig.1). Due to lack of instrumental records the epicenter location is not well determined. Based on field observations and ground excavation in the 1819 fault scarp, Rajendran et al. (1998) suggested a low angle reverse faulting for this earthquake analogous to the 1956 Anjar earthquake ( $M_L$  6.1) in the Kutch basin. They argued that the epicenter of the 1819 event was about 10 km north of the 'Allah Bund' (Fig.1). Paleoseismological evidences suggest that several pre-historic large earthquakes occurred in the region (Rajendran et al., 1988; Rajendran and Rajendran, 2001). The other significant earthquakes near to the study region are the 1969 Mt. Abu earthquake (M 5.3) and the 1970 Broach earthquake (M 5.4). Fault-plane solutions of these earthquakes also show reverse faulting with strike-slip component (Fig.1). Chandra (1977) interpreted left-lateral strike-slip movement for these earthquakes.

## MAIN SHOCK

The January 26, 2001 crustal earthquake ( $M_w$  7.6 + 0.1) in Bhuj, western India is one of the most deadly and well reported intraplate earthquakes (e.g. Gupta et al., 2001; Bendick et al., 2001). Teleseismic body waves were inverted to understand source mechanism and to map slip on the fault (e.g. Yagi and Kikuchi, 2001; Mori, 2001; Antolik and Dreger, 2003). Source mechanism of the main shock studied by different groups are given in Fig.2. The inversion of the wave forms studied by the ERI group (Yagi and Kikuchi, 2001) suggests that the slip occurred on a steeply dipping thrust fault, but it did not break the surface (Bendick et al., 2001). The moment tensor solution reported by the USGS and the P-wave first-motion fault-plane solution reported by the IMD (2002) are comparable with the ERI solution (Fig.2). The moment magnitude ( $M_w$ ), estimated by different organizations, ranges from 7.5 to 7.7 suggesting a rupture of 15-30 km width, 50-100 km length and average slip 4-6 m. Surface manifestation of such rupture is likely to be a broad zone of distributed uplift and subsidence with secondary surface faulting and cracking (Wesnousky et al., 2001).

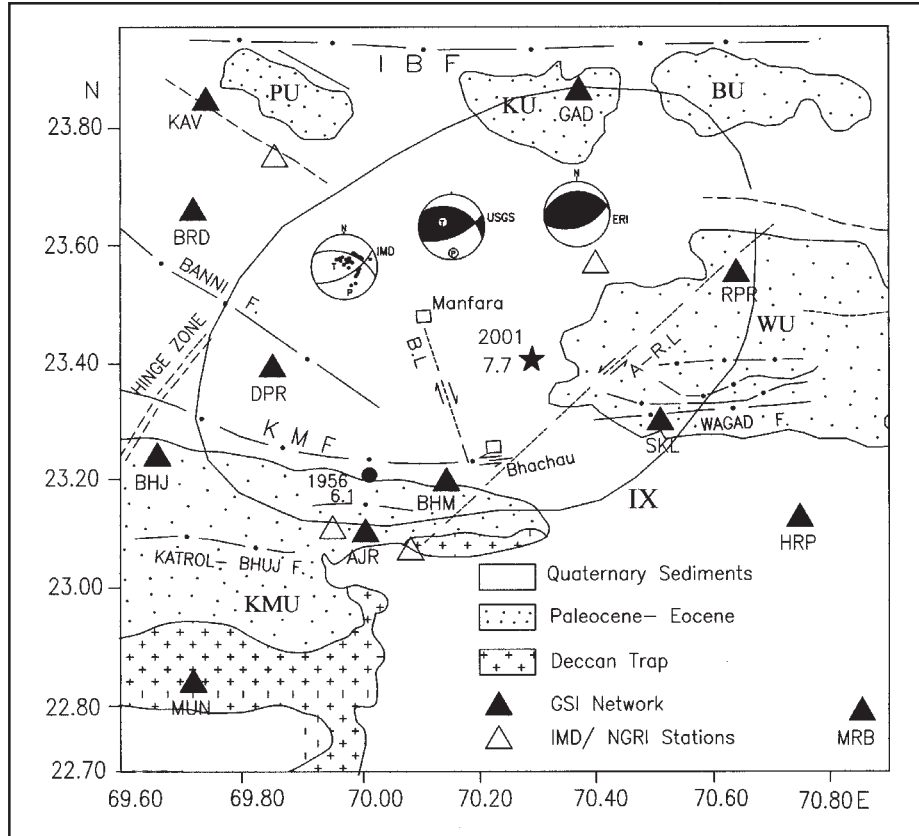


**Figure 2.** Detailed geology and the temporary seismic station locations are shown. ARL: Anjar Rapar Lineament, BL: Bhachau Lineament, WU: Wagad Uplift, BU: Bela Uplift, KU: Khadir Uplift, PU: Pachham uplift, KMU: Kutch Mainland Uplift. The high intensity zone, isoseismal IX, is shown. A few IMD and NGRI stations near the GSI network are also indicated. Fault-plane solutions of the main shock as reported by the ERI, USGS and IMD are shown (see text).

*Gahalaut and Bürgmann (2004)* analysed pre- and post- earthquake satellite images of the epicentral region, and suggested that maximum uplift is located about 15 km north of the main shock epicenter. Comparison of GPS-1997 and GPS-2001 coordinates at Jamnagar, that lies 150 km south of the main shock epicenter, gives the coseismic displacement vector of  $16 + 8$  mm at  $N35^{\circ} E$ ; this is the only GPS-GPS based estimate of coseismic slip of the Bhuj earthquake (*Jade et al., 2002*). *Chandrasekhar and Mishra (2002)* and *Chandrasekhar et al. (2004)*, based on repeat microgravity and geodetic measurements, reported maximum uplift of  $1.57 + 0.5$  m and a corresponding gravity change of  $-393 + 18$  mGal in the epicenter region. In a recent work on gravity and magnetic data, *Mishra et al. (2005)* delineated major E-W and NW-SE oriented faults and deep crustal inhomogeneity in the epicenter region.

*Singh et al. (2004)* studied source time function (STF) and radiated seismic energy ( $E_R$ ) using the

empirical Green's function (EGF) technique. They reported STF as a function of azimuth and nearly constant duration of 18 sec. The estimated  $E_R$  is  $2.1 \times 10^{23}$  erg and the corresponding estimate of slip velocity at the centre of the fault is 156 cm/sec. They also reported a high static stress drop of 200 bar which is a common feature for large intraplate earthquakes.

The main shock was well recorded by 13 strong-motion seismograph stations at a distance from 40 to 290 km from the epicenter (*IMD, 2002*). The spatial variation of the PGA (Peak Ground Acceleration) was estimated; it was 0.55g at the nearest (43 km) station at Anjar (rock) and 0.04g at Anand (alluvium) at a distance of 290 km. The Ahmedabad station (alluvium) recorded 0.13g at a distance of 240 km. It may be noted that many reinforced concrete frame buildings in the Ahmedabad city collapsed. The earthquake had left behind a large stock of buildings in the Bhuj and adjoining Ahmedabad area, which needed retrofitted and safety evaluation.

Seismotectonics of the 2001 Bhuj earthquake (Mw 7.7) in western India:  
Constraints from aftershocks

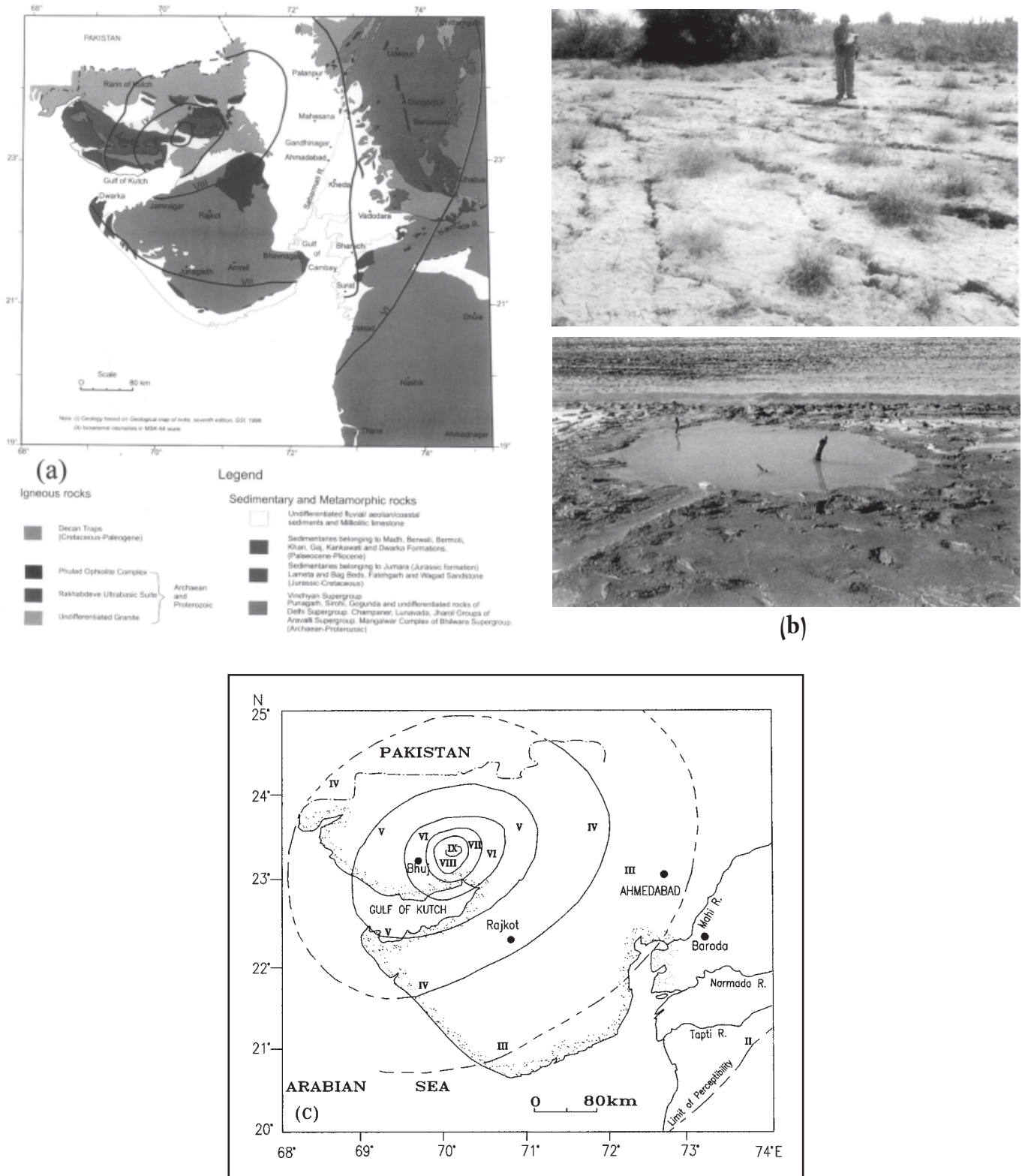


**Figure 3.** (a) Detailed geology of the study region and isoseismal intensity map of the January 26, 2001 Bhuj earthquake (after Pande et al., 2003). (b) Ground cracks and liquefaction in the intensity zone VIII (after Rajendran et al., 2001). (c) Isoseismals of the 1956 Anjar earthquake.

Intraplate earthquakes are though much complex, unlike the interplate earthquakes, some parallels have been reported between the 2001 Bhuj earthquake and the 1811-1812 New Madrid earthquakes ( $M_w$  7.5-8.0) that struck the central United States two centuries ago (e.g. *Hough et al., 2002; Schweig et al., 2003*). Though it is not clear whether the strain rates and the tectonic settings of the two regions are analogous, but both the intraplate Bhuj earthquake and the largest New Madrid event of February 7, 1812 occurred on paleo-rift thrust fault(s) in the lower crust, that did not manifest surface rupture (e.g. *Jhonston, 1996; Mueller and Pujol, 2001*). According to recent reinterpretation, the magnitudes of these two events may have been similar (*Hough et al., 2002*).

**ISOSEISMAL INTENSITIES**

Macroseismic survey was carried out immediately after the main shock, and several reports were available (e.g. *Ravishanker and Pande, 2001; Rastogi, 2001; Wesnousky et al., 2001; McCaplin and Thakkar, 2001; Rajendran et al., 2001*). A detailed report was then published by the Geological Survey of India (*GSI, 2003*). The earthquake caused a maximum intensity of X (MSK Scale) in an area of 780 sq.km. (Fig.3a). The inhabitants narrated that just before the severe ground shaking there was an explosion or deep rumbling sound.

Destruction of civil structures, irrespective of class or type of construction, was near total in the meizoseismal area, isoseist X. The isoseist IX comprised an area of 10,455 sq km (*Ravishanker and Pande, 2001*). In this zone also, many of the well built structures failed totally. No primary surface rupture was reported. *Wesnousky et al. (2001)*, however, reported a 8 km long secondary rupture along the Bhachau lineament; they called it Manfara rupture which passes through the Manfara town (Fig.2); the rupture showed right lateral motion upto 32 cm of slip. They have also reported a scarp, about 50 cm high, that strikes east-west over several hundred meters or more along the strike. About 100 m south of the scarp, the ground was pervasively fractured by extensional cracks (Fig.3b).

Profuse liquefaction in an area of about 50,000 sq km was reported in the form of sand blows/boils, craters, ground fissures, slumps etc. (*Ravishanker and Pande, 2001; Rajendran et al., 2001*). The sandy plains of Rann of Kutch and the Little Rann, where groundwater level was at shallower depths, have provided the most conducive environment for liquefaction in intensity zones VIII and above (Fig.3b).

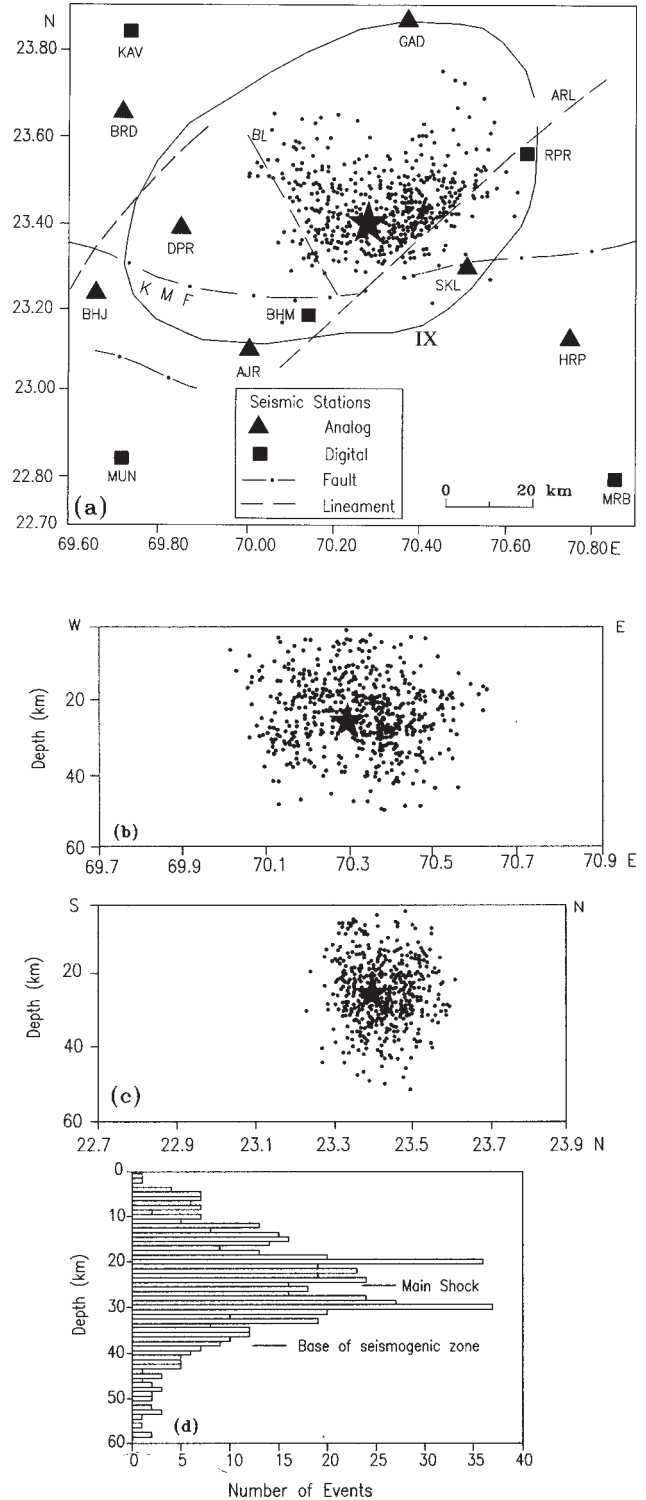


**Figure 4.** (a) Epicenter map of the 560 relocated events along with the location of the main shock (star) are shown, other details are as in Fig.2. (b) E-W and (c) N-S depth sections showing aftershocks and the main shock. (d) Histograms showing number of aftershocks at 1 km depth interval.

They have also reported coseismic secondary fractures cutting across the road surface, near the epicenter, with left-lateral displacement. Based on the isoseismal geometry, *Ravishanker and Pande (2001)* suggested that the main shock rupture propagated to the northeast.

## AFTERSHOCK DATA ANALYSIS

Precise locations of the aftershocks and fault-plane solutions play an important role to understand the rupture area and the seismogenic fault(s) in the source area. An attempt was first made to incorporate the aftershock data from various seismic stations operated in the epicentral zone by different national organizations for locations (Fig.2). The results were, however, not encouraging, possibly because of low precision data due to lack of synchronization of the clocks in the other local seismic stations, and we had no option to recheck these data with the original seismograms. Further, those seismic stations were run for smaller time periods and were established much later, after about two weeks of the main shock. Thus, we used the 12 – station GSI network data that were systematically recorded by all the stations for about two and a half months immediately after the main shock. The GSI network azimuthally covers well the main shock epicenter region (Fig.2). These were thoroughly scanned and were fairly sufficient for inversion for precise locations and for fault-plane solutions. The network and the detailed geology of the study area are shown in Fig.2.

Preliminary locations of the aftershocks are made using the Hypo 71 program of *Lee and Lahr (1975)* and the 1-D velocity model estimated by *Kayal et al. (2002a)*. About 800 events ( $M > 2.0$ ) were selected on the basis of preliminary analysis. These 800 events had an average rms error  $< 0.5$  sec in the preliminary analysis. In the next step simultaneous inversion using the classical Fortran source code SIMULPS12, developed by *Thurber (1983)* and later modified by *Eberhart-Phillips (1993)*, was used for estimation of 3-D velocity structure and joint determination of the hypocenter parameters (*Mukhopadhyay and Kayal, 2005*).

Out of about 800 events, 560 are relocated by simultaneous inversion. In the preliminary locations, using Hypo71 with the 1D velocity model, the average rms error was 0.5 s for the 800 events, and a large number of events were located with depth fixed at the initial value. In the simultaneous inversion method, the average rms error for the 560 relocated events was reduced to 0.19 s. The average error estimates in latitude, longitude and depth for these events are 1.2

km, 1.1 km and 2.3 km respectively. The relocated epicenters, two selected cross sections and frequency of aftershocks versus depth are shown in Fig.4.

Fault-plane solutions of the aftershocks reported by *Kayal et al. (2002a)* and by *De et al. (2003)* are re-examined. The best located events were selected for fault-plane solutions. Spatial, temporal and depth variations of the aftershocks are considered for the solutions, 10 well constrained solutions are illustrated in Fig. 5.

## RESULTS

### Aftershocks

The epicenters of the 560 relocated events show that the main shock as well as most of the aftershocks occurred to the north of the Kutch Mainland Fault (KMF) and within a V shaped zone delimited by the Bhachau Lineament (BL) to the west and by the Anjar Rapar Lineament (ARL) to the east (Fig.4a). The aftershocks occurred in an area with a maximum length of 70 km in the east-west and 35 km in the north-south. Two intense clusters of aftershocks, one to the northeast and one to the northwest, on both sides of the main shock, are observed.

Two cross sections of the aftershocks, one along east-west and the other along north-south, are illustrated in Figs. 4b and c. In the east-west section, two major clusters of aftershocks flanked both sides of the main shock. In the north-south section a steeply south dipping plane is envisaged. The frequency of aftershocks versus depth is shown in Fig.4d. It is observed that the base of the seismogenic zone lies at about 37 km, while the main shock occurred at 25 km depth. Most of the aftershocks occurred within 12 to 37 km depth range. A bimodal distribution of the aftershocks, above and below the main shock, is also observed.

### Fault-plane Solutions

Moment-tensor solution of the main shock (USGS) and 10 composite fault- plane solutions of the best located aftershocks are shown in Fig. 5. The best located epicenters clearly show two trends of the aftershocks, one northeast and one northwest. The composite fault-plane solutions are obtained for the clusters of aftershocks along the two trends at different depth levels. The fault-plane solutions vary for the two trends, and also vary with depth (Fig.5). We have further examined the source processes of the aftershocks at two time intervals; five solutions are obtained for the sequence in February 2001, and five

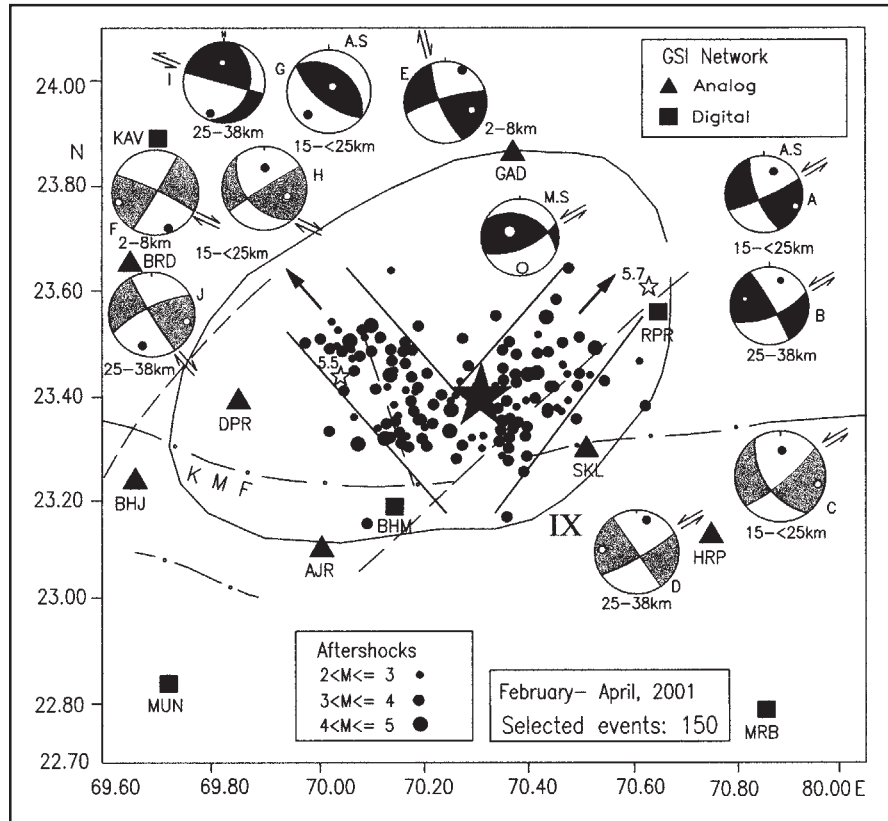


**Figure 5.** Fault-plane solutions of the main shock (MS) and the selected aftershocks (AS), (see text). In fault-plane solutions, shaded area indicates zone of compression and open area zone of dilatation; the darker shades for the February, 2001 sequence and lighter shade for the March – April, 2001 sequence; the solid circles indicate P-axes and open circles T-axes, (compiled from Kayal et al., 2002a and De et al., 2003). Two largest aftershocks (M 5.7 and M 5.5) located by the *IMD* (2002) are also shown.

solutions for the sequence in March-April, 2001. These solutions of two time periods are illustrated symbolically in Fig.5. Detailed first-motion plots are given by *Kayal et al. (2002a)* and by *De et al. (2003)*.

The main shock shows a reverse faulting with a left-lateral strike-slip motion along the east-northeast trending south dipping inferred fault plane (Figs 2 and 5); the inferred fault plane is supported by the south dipping plane envisaged in the north-south cross section of the aftershocks (Fig. 4c). Four composite solutions (A-D) for the northeast trending aftershocks, that occurred in the mid crust (depth 15-<25 km) and in the lower crust (depth 25-38 km), also show reverse faulting with left-lateral strike-slip motion along the northeast trending inferred fault. There is no much change in the fault-plane solutions with time and with depth; the solutions are fairly consistent. It may be noted that there was almost no event at a shallower depth (<10 km) in the northeast for a fault-plane solution.

Six composite solutions (E-J) are obtained for the northwest trending aftershocks that were recorded during February – April, 2001 (Fig.5). A few upper crustal (depth 2-8 km) aftershocks were recorded in the northwest, two composite fault-plane solutions (E and F) indicate reverse faulting with right-lateral strike-slip motion along the northwest trending inferred fault. There is no much change in the solutions (E-F) with time. At the mid crustal depth (15-<25 km), the northwest trending aftershocks recorded during February, 2001, show dominantly reverse faulting (solution G), but the later aftershocks recorded during March – April, 2001, on the other hand, show reverse faulting with right-lateral strike-slip motion (solution H). In the lower crust, at 25 – 38 km depth, the solution of the aftershocks of February, 2001 shows left-lateral strike slip (solution I), and the aftershocks of March – April, 2001 show right-lateral strike-slip (solution J). It may be noted that all the fault-plane solutions show NNE-SSW compressional stress.



## DISCUSSION AND CONCLUSIONS

The Bhuj earthquake is a paleorift-zone earthquake, which occurred at a deeper depth (25 km) compared to common shallower (10 - 15 km) intraplate events. The deeper Bhuj earthquake source zone in the Kutch rift basin is comparable with that of the deep focus (35 km) 1997 Jabalpur earthquake (M<sub>w</sub> 6.0) in the Narmada rift basin in central India (Kayal, 2000). The well recorded large data set of the Bhuj earthquake sequence, however, provided an opportunity for simultaneous inversion for precise locations of the events. The large sequence of the aftershocks also provided well constrained fault – plane solutions which are examined with space, time and depth.

Yagi and Kikuchi (2001) modelled the Bhuj earthquake deformation along a reverse fault having a 75 km x 35 km rupture plane with a maximum dislocation of 8.5 m at 23 km depth. Mori et al. (2001) reported that the fault area delineated by the aftershock activity for this earthquake is comparatively smaller for a main shock of M<sub>w</sub> 7.7 (Fig.1). On the basis of waveform inversion they proposed that the main shock hypocenter lies close to the largest area of slip, which is 10 x 20 sq km in size with a maximum slip of about 10 m. In a high resolution seismic tomography study, it is reported that the Bhuj earthquake source area falls within the high V<sub>p</sub> and high V<sub>p</sub>/V<sub>s</sub> zone (Kayal et al., 2002b), and it is an uplifted block (Mandal et al., 2004; Mukhopadhyaya and Kayal, 2005). Mori et al. (2001) identified this zone as an asperity, and argued that the asperity extends both upward and downward from the hypocenter. This suggestion, based on waveform inversion, supports the observation of the aftershock distribution (Fig. 4d), which indicates that the rupture propagated both upward and downward from the main shock hypocenter.

Negishi et al. (2002), based on aftershock data, reported that the depth range of faulting is 10-35 km; the main shock and the aftershocks occurred on buried fault(s). The deeper source zone of the Bhuj earthquake is very much evident from the intense aftershock activity (81%) at a depth range 12 – 37 km (Fig.4c). It is, however, interesting to note the bimodal distribution of the aftershocks with peaks at 20 km and at 30 km, 5 km above and below the main shock hypocenter (Fig.4d). The base of seismogenic zone is envisaged at 37 km (Fig.4d). Sibson (1986) and Lay and Wallace (1995) suggested that rupture for large crustal earthquake initiates at the base of a seismogenic zone. Such an observation was made for the 1997 Jabalpur earthquake (M<sub>w</sub> 6.0) in the Narmada rift basin in central India; it occurred at the base of

the seismogenic zone at a depth of 35 km and a downward rupture was reported (Kayal, 2000). The Bhuj earthquake was, however, initiated at a shallower (25 km) depth compared to the base of the seismogenic zone at 37 km. The bimodal distribution of the aftershocks suggests that the Bhuj earthquake rupture initiated in the mid-crust, and it propagated both down-dip near to the Moho, and up-dip, but not to the surface. The bimodal distribution of the aftershocks was also reported by Horton et al. (2001) and Bodin and Horton (2004), and they explained that such distributions are caused due to layered crustal rheology.

Further, the aftershock epicenters show a 'V' shaped area (Fig. 4a); a similar observation was reported by Wesnousky et al. (2001), (Fig.1). Within the V shaped aftershock area, two intense clusters of aftershock epicenters are observed, one in the northeast and the other in the northwest of the main shock (Fig. 4a); this is more evident with the best located larger events (Fig.5). It may be noted that the IMD (2002) located two largest aftershocks (M 5.7 and 5.5) immediately after the main shock, one to the northeast and one to the northwest (Fig.5); this observation supports the suggestion that the main shock rupture propagated to the northeast as well as to the northwest. Although no primary surface evidence of rupture was reported, surface manifestations were observed in the form of liquefaction and secondary ruptures, both in the northeast and in the northwest of the main shock epicenter (Ravishanker and Pande, 2001; Karanth et al., 2001; Rajendran et al., 2001; Wesnousky et al., 2001). Multifractures and fault interactions for large intraplate earthquakes are common (Talwani and Gangopadhyay, 2001.).

Kayal et al. (2002b) reported a number of crustal blocks based on the seismic velocity images. Mandal et al. (2004) and Mukhopadhyay and Kayal (2005) reported uplift of a high velocity block in the epicenter region. A gravity study in the area supports a block tectonics in the region (Chandrasekhar and Mishra, 2002). The regional isostatic anomaly suggests larger thickness of sediments towards south and general uplift of the basement towards north of the KMF, descending stepwise towards the south indicating post-rift vertical tectonics (Chandrasekhar and Mishra, 2002). Based on the analysis of gravity data, Chandrasekhar et al. (2004) further suggested that there are basement uplifts controlled by reverse faults with about 2-5 km upthrow in this region. Pre- and post- earthquake geodetic measurements show a maximum uplift of 1.57 + 05 m in the epicenter region (Chandrasekhar and Mishra, 2002). Gahalaut

and Bürgmann (2004) analysed pre- and post-earthquake satellite images of the epicentral region. They suggested a maximum uplift is located about 15 km north of the epicenter.

Lateral heterogeneity as well as complex velocity structure, a high velocity and low velocity contact zone at a shallow depth (7 km + 1 km), was reported to be the source area for the 1993 Killari earthquake ( $M_w$  6.3), a damaging intraplate earthquake in central India (Kayal and Mukhopadhyay, 2002). Hauksson and Haase (1994) reported four earthquakes ( $M > 5.9$ ) in the Los Angeles basin, California, at the boundary between low and high velocity zones; they interpreted that the high velocity zone forms the upper block of a thrust fault. A similar observation was reported for the 2001 Bhuj earthquake source area (Kayal et al., 2002b; Mandal et al., 2004; Mukhopadhyay and Kayal, 2005), and it is supported by gravity and magnetic observations (Chandrasekhar and Mishra, 2002; Mishra et al., 2005).

Kayal et al. (2002b) inferred that the rocks of lower rigidity or the fluid-filled rock matrix might have contributed to the initiation of the Bhuj main shock. Zhao et al. (2002) reported the role of fluid/magma filled rocks in nucleation of earthquakes in Japan. Mishra and Zhao (2003) reported high crack density, high porosity and high saturation in the Bhuj earthquake source area. Ray (2004), on the other hand, suggested that activation of a fault that causes a large earthquake generates enough flush heat to melt the fragmented rocks at the frictional interfaces. The block structures, velocity heterogeneity and melt rock (?) / fluid filled rock (?) in the source area are, however, studied after the main shock. The fluid filled (?) or melt rock (?) in source area may, however, be a pre-earthquake or a post – earthquake phenomena. This phenomena can not be resolved unless both the pre-earthquake (main shock) and post earthquake tomography studies are made.

The Kutch paleorift basin comprises of a series of uplifts, master faults and up-thrusts (Fig. 1). Biswas (1987) postulated that the uplifts are the result of the differential movements of discrete basement blocks due to compression along these faults. Ravishanker (1995) suggested that differential thermal and crustal structures provide the motive force for relative movements between various crustal block under the NNE-SSW compressive stress due to northward movement of the Indian plate. Pre-earthquake and post-earthquake gravity and magnetic study confirmed a block uplift in the source area (Chandrasekhar and Mishra, 2002; Mishra et al., 2005). A coseismic displacement of 16+8 mm at N35°E during the Bhuj earthquake is reported by Jade et al. (2002) from GPS

(1997) – GPS (2001) measurement at Jamnagar which is about 150 km south of the main shock epicenter, and lies on the hanging wall of the reverse fault that caused the earthquake. This indicates that the post seismic deformation controls this shortening. They further reported shortening of the baseline lengths of five GPS points within the KRB irrespective of their orientation relative to the NNE-SSW compressional direction. The dominant NNE-SSW compressional stress is evident in the fault-plane solutions of the main shock and aftershocks (Fig.5).

The fault-plane solutions of the main shock and aftershocks support the upward reverse movement in the source area (Fig.5). The main shock shows reverse faulting with a left-lateral strike-slip motion along the south dipping ENE-WSW trending inferred fault. The northeast trending aftershocks also show reverse faulting with left-lateral strike-slip motion at the mid crust (15-<25 km) as well as at the lower crust (25-38 km) along the inferred fault. There is no much change in mechanisms (A-D) of the aftershocks with depth or with time for the northeast trending aftershocks (Fig.5). Almost all the aftershocks occurred at the mid-crust and lower crust, and these events occurred dominantly by reverse faulting with left-lateral motion, comparable with the main shock solution. We believe that the northeast trending aftershocks occurred by the main rupture at the main shock depth level. The northwest trending aftershocks, on the other hand, show different solutions; these solutions vary with depth and also with time. At the lower crust (25 – 38 km), reverse fault solutions with left-lateral strike-slip as well as with right-lateral strike-slip are obtained (solutions I and J respectively). At the mid-crust (15-<25 km) a pure reverse faulting and a thrust faulting with right – lateral slip are obtained (solutions G and H respectively). At the upper crust (2-8 km), the two solutions (E and F) show almost consistent right-lateral strike-slip (Fig. 5). We suggest that the aftershocks along the northwest were generated by conjugate fault(s) which show dominantly reverse faulting with right-lateral slip, except one (solution I) at the lower crust (25-38 km) that shows left-lateral motion and one at the mid-crust that shows pure reverse faulting (solution G) for the sequence in February, 2001. The NNE-SSW compressional axis of all the solutions is consistent with the regional stress due to north-northeast movement of the Indian plate.

Ground observations along the two known surface lineaments are compatible with the above fault-plane solutions. Wesnousky et al. (2001) reported a

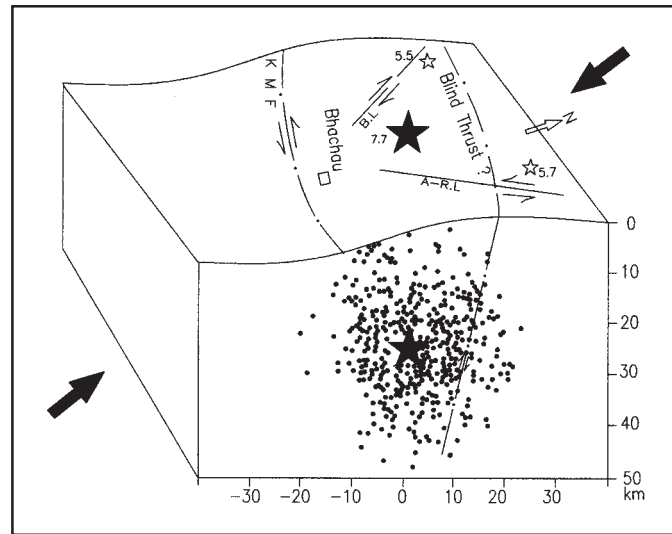


**Figure 6.** A schematic seismotectonic model of the Bhuj earthquake sequence. The depth section of the aftershocks is taken from Fig. 4c.

northwest striking 8 km long secondary rupture with a right-lateral strike-slip showing a maximum offset of 32 cm. *Ravishanker and Pande (2001)*, based on the isoseismal geometry (Fig.3), suggested that the main rupture propagated towards northeast, and reported left-lateral ground motion along the ARL. They also reported right-lateral ground motion along the Bhachau lineament. *Pande (2003)* further reported that the isoseismal trend of the intensities IX and VIII corresponds to the Delhi – Aravalli structural grain, and he suggested that the causative fault could be parallel to this Precambrian fold belt pattern. The isoseismals of the 1956 Anjar earthquake also showed similar elongation (Fig.3c). The isoseismal VII of the 2001 Kutch earthquake, after maintaining a fair degree of parallelism with the isoseismals in the Saurashtra region, abruptly adopts a N-S trend in the Mainland Gujarat. This conspicuous swing is attributed to the trend of CRB (*Pande, 2003*). *Mishra and Zhao (2003)* reported that the fracture along northeast had higher degree of saturation. These observations support our suggestion that the main rupture propagated along the northeast and a conjugate rupture to the northwest; this observation illustrated by a fault interaction model (Fig.6). We suggest that these two ruptures caused a V shaped aftershock area (Figs 1 and 5).

There is no mapped fault along the surface projection of the inferred seismogenic fault (*Negishi et al., 2002; Kayal et al., 2002a*). The aftershocks are mostly confined to deeper depths (12-37 km). A similar observation of the 1811-12 New Madrid large earthquake was reported; these findings suggest that

such large intraplate earthquake can occur by hidden fault(s) without producing surface rupture. The main shock and the aftershocks occurred in a high velocity block filled with fluid (?), this is similar to that observed in other large earthquakes in the world (*Mendoza and Hartzell, 1988; Zhao et al., 2004*). The precise locations and fault-plane solutions provide a new insight into the Bhuj earthquake source processes. The rupture propagation and different fault-plane solutions with depth, space and time are well reflected by the aftershocks.

#### ACKNOWLEDGEMENT

JRK is thankful to the Director General, GSI, for his kind permission to publish the work. We are thankful to Dr. Harsh K. Gupta for his kind invitation and encouragement for this review work.

#### REFERENCES

- Antolik, M. and Dreger, D.S. 2003. Rupture process of the 26 January, 2001  $M_w$  7.6 Bhuj, India earthquake from teleseismic broadband data, *Bull. Seism. Soc. Am.*, 93, 1235-1248.
- Bendick, R., Bilham, R., Fielding, E., Gaur, V.K., Hough, S.E., Keir, G., Kulkarni, M.N., Martin, S., Mueller, K. and Mukul M., 2001. The 26 January "Republic Day" Earthquake, India, *Seism. Res. Lett.*, 72(3), 328-335.
- Biswas, S.K., 1987. Regional tectonic framework, structure and evolution of the western marginal basins of India, *Tectonophysics*, 135: 307-327.
- Bodin, P. and Horton, S., 2004. Source Parameters and

- tectonic implications of Aftershocks of the  $M_w$  7.6 Bhuj earthquake of 26 January 2001, *Bull. Seism. Soc. Am.*, 94: 818-827.
- BIS (2002). Seismic Zoning Map of India, Bureau Indian Standard publication.
- Chandra, U., 1977. Earthquakes of Peninsular India – A seismotectonic study, *Bull. Seism. Soc. Am.*, 67, 1387-1413.
- Chandrasekhar, D.V. and Mishra, D.C., 2002. Some geodynamic aspects of Kutch basin and seismicity: Insight from gravity studies, *Curr. Sci.*, 83(4) : 492-498.
- Chandrasekhar, D.V., Mishra, D.C., Singh, B., Vijayakumar, V. and Burgmann, R., 2004. Source parameters of the Bhuj earthquake, India of January 26, 2001 from height and gravity changes, *Geophys. Res. Lett.*, 31, L19608.
- De, R., Gaonkar, S.G., Srirama, B.V., Saginaram and Kayal, J.R., 2003. Fault plane solutions of the January 26<sup>th</sup>, 2001 Bhuj earthquake sequence, *Earth Planet Sci. (Proc. Indian Acad Sci)*, 112(3), 1-7.
- Eberhart-Phillips, D., 1993. Local earthquake tomography: Earthquake source region: In: Seismic Tomography: Theory and practice, ed. H.M. Iyer and K. Hirahara, Chapman and Hall, London, P. 613-643.
- Gahalaut, V.K. and Burgmann, R. 2004. Constraints on the source parameters of the 26 January, 2001 Bhuj earthquake from satellite images, *Bull. Seism. Soc. Am.*, 96(6), 2407-2413.
- GSI, 2000. Seismotectonic Atlas of India and its Environs, *Geol. Surv. India Sp. Pub.* Calcutta.
- GSI, 2003. The January 26, 2001 Bhuj Earthquake, Ed. P. Pande and J.R. Kayal, *Geol. Survey India Sp. Publication* v.73; 300p.
- Gupta, H.K., Rao, N.P., Rastogi, B.K. and Sarkar, D., 2001. The deadliest intraplate earthquake, *Science*, 291, 2101-2102.
- Gutenberg, B. and Richter C.F., 1954. Seismicity of the Earth, *Princeton University Press, New Jersey*, 310p.
- Hauksson, E and Haase, J., 1994. Three dimensional Vp and Vp/Vs velocity models of the Los Angeles basin and central Transverse ranges, California, *J. Geophys. Res.* 102, 5423-5453.
- Hough, S.E., Stacey, M., Bilham, R., Atkinson, G.M., 2002. The 26 January 2001 M 7.6 Bhuj India earthquakes: observed and predicted ground motions, *Bull. Seism. Soc. Am.*, 92, 2061-2079.
- Hurton, S., Bodin, P., Johnston, A., Patterson, G., Bollwerk, J., Rydelek, P., Raphael, A., Chiu, C. Chiu, J-m, Busdhabatti, K. and Gomberg, J., 2001. Bhuj aftershocks recorded by the MAE/ISTAR temporary seismic network, Int. Conf. Seismic Hazard with particular reference to Bhuj earthquake of January 26, 2001, IMD-DST, New Delhi, Oct. 3-5, 2001. Abs. Vol., 103-104.
- IMD, 2002. Bhuj Earthquake of January 26, 2001, a consolidated document, *Unpub. Report*, Seismology No. 3/2002, 131P. IMD, New Delhi, 120P.
- Jade Sridevi, Mukul, M., Parvez, I.A., Ananda, M.B., Kumar, P.D. and Gaur, V.K., 2002. Estimates of coseismic displacement and post seismic deformation using global positioning system geodesy for the Bhuj earthquake of 26 January, 2001. *Curr. Sci.*, 82(6), 748-752.
- Johnston, A.C., 1996. Seismic moment assessment of earthquakes in stable continental regions I. *Geophys. J. Int.*, 124 : 281-414.
- Johnston, A.C. and Kanter, L.R., 1990. Stable continental earthquakes, *Sci. Am.*, 262 : 68-75.
- Karanth, R.V., Sohoni, P.S., Mathew, G. and Khadikar, A.S., 2001. Geological observations of the 26 January, 2001 Bhuj earthquake, *J. Geol. Soc. India*, 58, 193-202.
- Kayal, J.R., 2000. Seismotectonic study of the two recent SCR earthquakes in central India, *J. Geol. Soc. India*, 55, 123-138.
- Kayal, J.R. and Mukhopadhyay, S., 2002. Seismic tomography structure of the 1993 Killari earthquake source area, *Bull. Seism. Soc. Am.* 92(5), 2036-2039.
- Kayal, J.R., De, R., Saginaram, Srirama, B.V., Gaonkar, S.G., 2002a. Aftershocks of the 26 January, 2001 Bhuj earthquake in western India and its seismotectonic implications, *J. Geol. Soc. India*, 59, 395-417.
- Kayal, J.R., Zhao, D., Mishra, O.P., De, R. and Singh, O.P., 2002b. The 2001 Bhuj earthquake: Tomography evidence for fluids at hypocentre and its implications for rupture nucleation, *Geophys. Res. Lett.* 29 (24), 51-54.
- Lay, T. and Wallace, T.C., 1995. Modern Global Seismology, *Academic Press, New York, USA*, 521p.
- Lee, W.H.K. and J.C., Lahr, 1975. HYPO-71: A computer program for determining hypocentre, magnitude and first motion pattern of local earthquakes. Open file report, *U.S. Geological Survey*, Revised Edition.
- Mandal, P., Rastogi, B.K., Satyanarayana, H.V.S. and Kousalya, M., 2004. Results from local earthquake velocity tomography: implications toward the source process involved in generating the 2001 Bhuj earthquake in the lower crust beneath Kachchh (India), *Bull. Seism. Soc. Am.* 94, 633-649.
- McCaplin, J.P. and Thakkar, M.G., 2003. 2001 Bhuj-Kachchh earthquake : surface faulting and its relation with neotectonics and regional structures, Gujarat, Western India, *Annals of Geophysics*, 46, 937-956.
- Mendoza, C. and Hartzell, S.H., 1988. Aftershock patterns and main shock faulting, *Bull. Seism. Soc. Am.* 78, 1438-1449.
- Mishra, D.C., Chandrasekhar, D.V. and Singh, B., 2005.

- Tectonics and crustal structures related to Bhuj earthquake of January 26, 2001 : based on gravity and magnetic surveys constrained from seismic and seismological studies, *Tectonophysics*, 396 : 195-207.
- Mishra, O.P. and Zhao, D., 2003. Crack density saturation rate and porosity at the 2001 Bhuj, India, earthquake hypocenter : a fluid driven earthquake ? *Earth and Planetary sci. Lett.*, 212, 393 - 405.
- Mori, J., Negishi, H. and Sato, T., 2001. Slip distribution of the 2001 West India earthquake from inversion of teleseismic data. Int. Conf. Seismic Hazard with particular reference to Bhuj earthquake of January 26, 2001, IMD-DST, New Delhi, Oct. 3-5, 2001. Abs. Vol.,
- Mueller, K. and Pujol, J., 2001. Three dimensional geometry of the Reeltoot blind thrust : implications for moment release and earthquake magnitude in the New Madrid Seismic zone, *Bull. Seism. Soc. Am.*, 91, 1563-1573.
- Mukhopadhyay, S., Kayal, J.R. and A. Kumar, 2002. Seismic Tomography of the Bhuj area using aftershocks of 26 January, 2001 earthquake, presented at 12<sup>th</sup> Symposium on Earthquake Engineering, IIT Roorkee, Dec. 16-18.
- Mukhopadhyay, S., Kayal, J.R., 2005. The 2001 Bhuj earthquake  $M_w$  7.7 in Western India : 3D velocity structure and seismotectonic model, *Tectonophysics* (Submitted).
- Negishi, H., Mori, J., Sato, T., Singh, R., Kumar, S. and Hirata, N., 2002. Size and orientation of the fault plane for the 2001 Gujarat, India earthquake Mw 7.7 from aftershock observations : A high stress drop event, *Geophys. Res. Lett.*, 29(20), 10-1-10.4.
- Oldham, R.D., 1926. The Cutch earthquake of 16<sup>th</sup> June, 1819 with a revision of the great earthquake of 12<sup>th</sup> June, 1897, *Mem. Geol. Surv. India*, 46 : 1-77.
- Pande, P., 2003. Seismotectonic frame work of the region and source mechanism of Kutch earthquake 2001; In : Kutch (Bhuj) Earthquake 26 January, 2004. Ed. P. Pande and J.R. Kayal, *Geol. Surv. Sp. Pub.* 76, 225-233.
- Pande, P., Kayal, J.R., Joshi, Y.C. and Ghevariya, 2003. Lithotectonic frame work of Gujarat and adjoining regions; In : Kutch (Bhuj) Earthquake 26 January, 2001. Ed. P. Pande and J.R. Kayal, *Geol. Surv. Sp. Pub.* 76, 5-9.
- Rajendran, C.P., Rajendran Kusala and John, Biju, 1998. Surface deformation related to the 1819 Kachchh earthquake : Evidence for recurrent activity. *Curr. Sc.*, 75, 623-626.
- Rajendran, C.P., Rajendran K., 2001. Characteristics of deformation and past seismicity associated with the 1819 Kutch earthquake, northwestern India, 91(3), 407-426.
- Rajendran, K., Rajendran, C.P., Thakkar, M., Tuttle, M. P., 2001. The 2001 Kutch (Bhuj) earthquake: Coseismic surface features and their significance, *Curr. Sci.*, 80(II), 1397-1405.
- Rastogi, B.K., 2001. Ground deformation study of Mw 7.7 Bhuj earthquake of 2001, *Episodes*, 24(3), 160-165.
- Ray, S.K., 2004. Melt-clast interaction and power law size distribution of clasts in Pseudotachylytes, *J. Str. Geol.* 26(10), 1831 – 1843.
- Ravishanker, 1995. Fragmented Indian shield and recent earthquakes, *GSI Sp. Pub.* 27, 41-48.
- Ravishanker and Pande, P., 2001. Geoseismological studies of Kutch (Bhuj) earthquake of 26 January, 2001, *J. Geol. Soc. India*, 58, 203-208.
- Schweig, E., Gomberg, J., Petersen, M., Ellis, M., Bodin, P., Mayrose, L., and Rastogi, B.K., 2003. The  $M_w$  7.7 Bhuj Earthquake: Global lessons for Earthquake Hazard in Intra-plate regions, *J. Geol. Soc. India*, 61, 277-282.
- Sibson, R.H., 1986. Earthquakes and rock deformation in crustal fault zones; *Ann. Rev. Earth Planet Sci.* 14, 149-175.
- Singh, S.K., Pacheco, J.F., Bansal, B.K., Perez-campos, X., Dattatrayam and Suresh G., 2004. A source study of the Bhuj, India Earthquake of 26 January, 2001 ( $M_w$  7.6), *Bull. Seism. Soc. Am.*, 94(4), 1195-1206.
- Talwani, Pradeep and Gangopadhyay, Abhijit, 2001. Tectonic framework of the Kachchh earthquake of January 26, 2001, *Seism. Res. Lett.*, 72 : 336-345.
- Thurber, C.H., 1983. Earthquake location and three dimensional crustal structure in the Coyote Lake area, Central California, *J. Geophys. Res.* 88, B10 : 8226-
- Wesnousky, S.G., Seeber, L., Rockwell, T.K., Thakur, V., Briggs, R., Kumar, S. and Ragona, D., 2001. Eight days in Bhuj: Field report bearing on surface rupture and Genesis of the 26 January, 2001 earthquake in India, *Seism. Res. Lett.*, 72(5), 514-524.
- Yagi, Y. and Kikuchi, M., 2001. Results of rupture process for January 26, 2001, Western India earthquake (Ms 7.9), (revised), <http://ll.wwweic.eri-u.Tokyo.ac.jp>
- Zhao, D., Hasegawa, A. and Horiuchi, S., 1992. Tomographic Imaging of P and S wave velocity Structure Beneath Northeast Japan, *J. Geophys. Res.*, 97 : 19,909 – 19,928.
- Zhao, D., Mishra, O.P. and Sanda, R., 2002. Influence of fluids and magma on earthquakes: Seismological evidence, *Phys. Earth Planet. Int.*, 132, 249-267.